ASTIGMATIC GAUSSIAN BEAMS in PLASMAS

S. Nowak, D. Farina, G. Ramponi

Istituto di Fisica del Plasma, Ass. EURATOM-ENEA-CNR
Via Cozzi 53, 20125 Milano, Italy

e-mail: nowak@ifp.cnr.it

The effects of astigmatic Gaussian beams on the width of narrow and well localized EC power deposition and driven current profiles are investigated in a reference ITER plasma by using the quasi-optical ECWGB code.

1. Introduction

In many experiments of ECRH/ECCD (as in those prone to neoclassical tearing modes stabilization) the launching system of EC waves is carefully designed to optimize the beam width in order to obtain narrow and well localized power deposition and/or driven current profiles with convergent mirrors. However, the reflecting surfaces, if characterized by two different focal lengths, can deform the circular beam coming from the waveguide and produce an astigmatic beam with different waist sizes and locations.

The aim of this work is to investigate the effects of astigmatic Gaussian beams (GBs) on the ECRH and ECCD profiles: these beams are modelled in a self-consistent way using the ECWGB quasi-optical code [1,2]: both astigmatic and circular GBs propagation can be described taking into account the beam self-diffraction through the complex eikonal equation.

The chosen target plasma is a typical ITER high β scenario [3]: the astigmatic divergent GBs are injected at 170 Ghz either from the equatorial and the top launcher.

In this paper the general modelling of the quasi-optical GBs propagation implemented in the ECWGB code is described in Sec. 2. In Sec. 3, the beam evolution in vacuum and in the target ITER plasma, starting from general launching conditions, is shown, and the beam cross-section deformation is investigated both in width and in axes orientation. In Sec. 4 the effect of astigmatic/circular beams on the width of the EC power and driven current profiles is discussed. In Sec. 5, short conclusions are presented.

2. General modeling of Gaussian beams

In the ECWGB code the complex eikonal equation $(\nabla S)^2 = n^2$ allows to describe the beam self-diffraction through its imaginary part, associated with the field amplitude. The eikonal function S(x) can be written in the antenna reference system (x',y',z'), being y' the propagation axis and x' parallel to the equatorial plane, as:

$$\operatorname{Re} S(x) = \frac{x'^2}{2R_x(y')} + \frac{z'^2}{2R_z(y')} + y', \quad \operatorname{Im} S(x) = \frac{x'^2}{w_x^2(y')} + \frac{z'^2}{w_z^2(y')}$$

$$w_i^2(y') = w_{i,0}^2\left[1 + \left(y' - y_{i,0}\right)^2 / L_i^2\right], L_i / R_i = \left(y' - y_{i,0}\right)/L_i + L_i / \left(y' - y_{i,0}\right) \ (i = x, z)$$

where $w_{i,0}$ and $y_{i,0}$ are the waist size and position, R_i the radius of curvature, $L_i=k_0 w_{i,0}^2/2$, and $k_0=\omega/c$.

The GB is described by a set of rays with initial conditions given in the antenna plane (Fig. 1). The initial coordinate of the rays in the (x',y',z') reference system are: $x'(j,k) = w_x \Delta\rho\,(j-1) \sin\theta_k$, $z'(j,k) = w_z \Delta\rho\,(j-1) \cos\theta_k$, $y'(j,k) = 0$, with $j=1,\ldots N_\rho$, $k=1,\ldots N_k$, $\Delta\rho=1/N_\rho$, the total number of rays being $N_t=N_\rho \times N_k + 1$. The initial launching components of the wave vector **k'** in the antenna system are expressed by: $k'_x / k'_y = x'/R_x$, $k'_z / k'_y = z'/R_z$, with $k'^2= k_0^2 (1+\nabla I^2)$, where ∇I is the gradient of Im(S). For $w_x=w_z=w$, a circular beam is described.

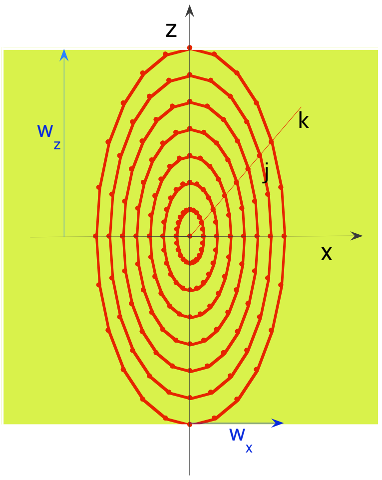

Fig.1–Initial ray positions in the antenna plane for an astigmatic GB.

The antenna system is rotated through the poloidal and equatorial angles, α and β respectively, defined in such a way that in the cylindrical reference system (used in the ECWGB code) the refractive index of the reference ray can be expressed by:

$$N_\varphi = \sin\beta,\ N_R = -\cos\beta\cos\alpha,\ N_z = -\cos\beta\sin\alpha$$

3. Gaussian beams propagation in vacuum and in plasma

We consider the propagation of GBs in a target ITER plasma for a typical scenario (Q=10, I_p=15 MA, β_p=0.65, li=0.70, B_{ax}=5.3 T, T_{e0}=24.8 keV, $n_{eo}=10^{20}$

m^{-3}). The beams are injected from two EC launchers located in the equatorial and upper ports, respectively.

In order to highlight the behaviour of the astigmatic beams, we consider GBs characterized in vacuum by two waist sizes of 1.5 and 3 cm at the same location in the antenna plane. Examples of evolutions of GBs, injected from the upper port with □=56.4° and □=20°, are shown for a circular and an astigmatic beam in Figures 2, 3, respectively. To investigate the beam deformation along the trajectory in vacuum and in plasma, we introduce a local reference system (x’, y’, z’) with the axis y’ corresponding to the local beamline direction, and the x’ axis still parallel to the equatorial plane. At each time step, the beam cross-section is projected on the plane y’=0, i.e. perpendicularly to the center beamline. Several contours of GBs, starting from the same launching plane, are compared in vacuum and in plasma at the same constant time steps.

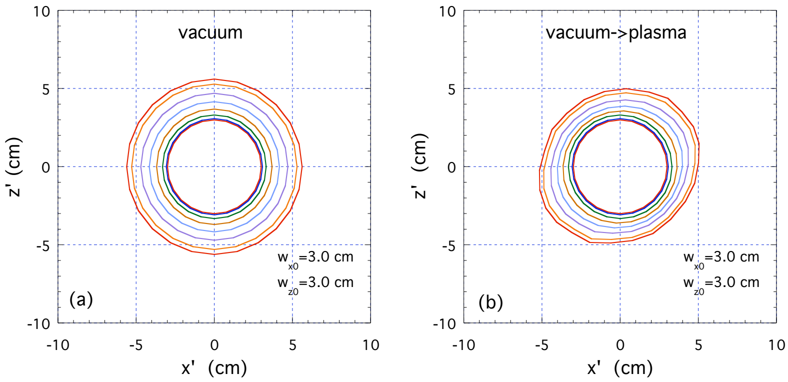

Fig.2–Circular beam evolution in vacuum (a) and in plasma (b) with $w_{x,0}= w_{z,0}$=3 cm.

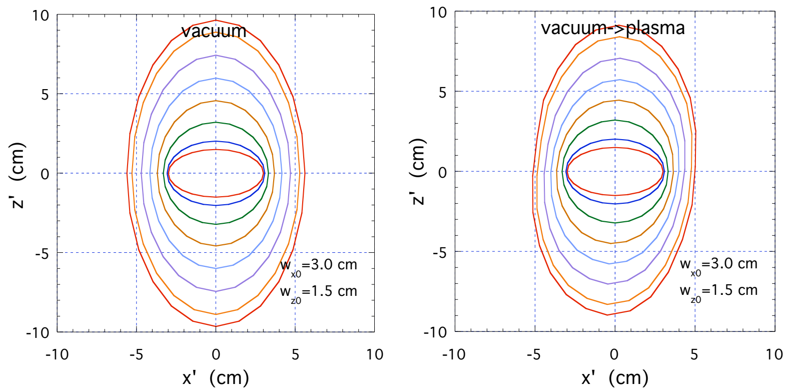

Fig.3–As in Fig.2 for an astigmatic beam with $w_{x,0}$=3 cm and $w_{z,0}$=1.5 cm.

Figures 2 and 3 show that the plasma induced astigmatism produces a small but finite beam cross section deformation either in width and axes orientation also for a circular beam. These effects depend on the specific trajectory. The cross sections of circular and astigmatic beams are compared at the same optical distance s from the launching point. The contours of two GBs ($w_{x,0}$=1.5 cm, $w_{z,0}$=3 cm and $w_{x,0}$=3 cm and $w_{z,0}$=1.5 cm) for top injection (□=56.4°) are shown both for □=0° and □=20° in Fig.4, at the antenna distance corresponding in plasma to the q=3/2 location.

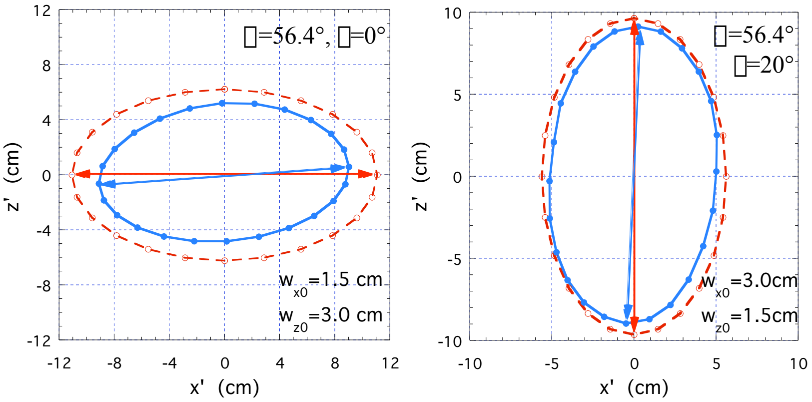

Fig.4–Beam contours of astigmatic beams from top launcher in vacuum (dashed lines) and in plasma (solid lines) for □=0° and □=20°, and s=260 cm and s=230 cm, respectively.

For the considered ray trajectories, either with □=0° and □=20°, the beam widths in vacuum are found larger than in plasma, where also a small axis rotation is produced. Therefore, the plasma effect on GBs propagation is to slightly deform their sections and rotate their axes. Plasmas more refractive than the considered one could increase the induced plasma astigatism.

4. Role of astigmatism on the ECRH/ECCD profiles width

The power deposition and the driven current density profiles have to be maintained narrow and well localized for many physical applications (as the NTMs stabilization at specific value of the safety factor q). Here, we investigate which local beam size (i.e., either w_x or w_z) plays a role on the profile width.

The beam shape effects on the power deposition and driven current profiles are investigate by injecting GBs from the midplane (R_A= 830 cm, z_A=0 cm, □=0°) and the top (R_A=695 cm, z_A=436 cm, □=56.4°) launchers, being R_A, z_A the antenna location coordinates. Perpendicular (□=0°) and oblique (□=20°) propagations of GBs, characterized by three different ratio $w_{z,0}$ / $w_{x,0}$ = 0.5, 1, 2, are considered for each launch in order to calculate and compare the ECH/CD profiles. In the ECWGB code the weakly relativistic EC power absorption and the relativistic current drive are computed along each ray of the beam. We summarize the results for the considered four beam injection in the Table below, where d_p is the power deposition profile full width at 1/e of its peak value, w_{xp} and w_{zp} the local beam sizes at the power peak location, and the normalized cartesian components of the gradient of the poloidal flux function □ (□□/|□□□|)$_p$ are given in the local reference system, at the same location.

Table

□	□	w_{x0} (cm)	w_{z0} (cm)	**d_p (cm)**	w_{xp} (cm)	w_{zp} (cm)	(□□/|□□□|)$_p$
0°	0°	3	3	**8.72**	5.9	7.0	(0, 0.999, -0.018)
		1.5	3	**8.78**	10.3	7.1	
		3	1.5	**8.72**	7.0	12.5	
0°	20°	3	3	**14.15**	6.5	6.2	(-0.44,0.89,0.06)
		1.5	3	**20.1**	10.6	6.3	
		3	1.5	**14.3**	6.6	10.7	
56.4°	0°	3	3	**5.61**	5.5	5.0	(-0.06, -0.11,0.99)
		1.5	3	**5.64**	9.0	5.0	
		3	1.5	**9.76**	5.5	9.8	
56.4°	20°	3	3	**8.44**	5.2	4.9	(-0.24, -0.56,0.79)
		1.5	3	**8.55**	8.9	4.9	
		3	1.5	**14.9**	5.2	9.0	

It is found that the obtained profile width variation is related to the variation of the waist w_{z0} in the case of top injection, and to that of w_{x0} in the equatorial and oblique injection cases. Note that the profiles are larger for the case of smaller waists, since beams with smaller waist are more divergent. Looking at the (□□/|□□□|)$_p$ components, it is found that the EC power profile width is determined by the local beam size corresponding to the larger □□ component in the (x', z') plane. The beam astigmatism does not play a role on the profiles for the equatorial and perpendicular launch, because □□ is parallel to the group velocity $\mathbf{v}_g$ (being zero the x and z components of □□, the change in w_x or w_z does not affect the profile width).

In Fig. 5, the beam shape effects on the power absorption profile are shown for the oblique GBs injection from top and equatorial ports. The same behaviour is found for the driven current profiles.

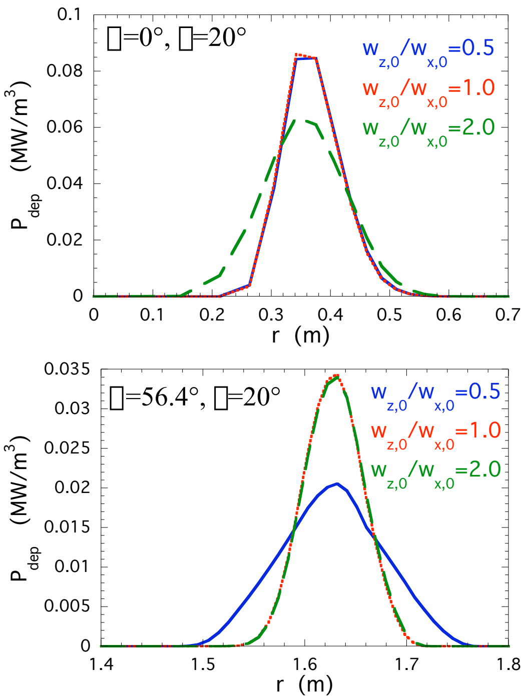

Fig.5–Power deposition profiles for oblique injection from midplane port (top) and from upper port (bottom), for three different waist ratios w_{z0}/w_{x0}=0.5, (solid line), 1 (dotted line), 2 (dashed line).

5. Conclusions

By using a general modeling of astigmatic Gaussian beams, we have shown that, for the chosen ITER scenario and wave frequency, the plasma-induced astigmatism produces a small but finite cross section deformation both in width and axes orientation.

We have investigated the beam shape effect on the ECRH/ECCD profile widths. We have found that the profiles modifications are determined by the change of the local beam size (either w_x or w_z) corresponding to the larger □□ component in the (x', z') plane. Astigmatism does not play a role on the width of the ECRH/ECCD profiles whenever the gradient of the poloidal flux function is parallel to the beamline direction (i.e., □□ // v_g).

References

[1] S.Nowak and A.Orefice, J. Plasma Phys., **57**, 349 (1997).
[2] D.Farina, S.Nowak, G.Ramponi, IFP Report FP **03/6** (October 2003).
[3] A.Portone and G.Saibene, http://efdsql.ipp.mpg.de/EUHandCD/ECRH/equilibria